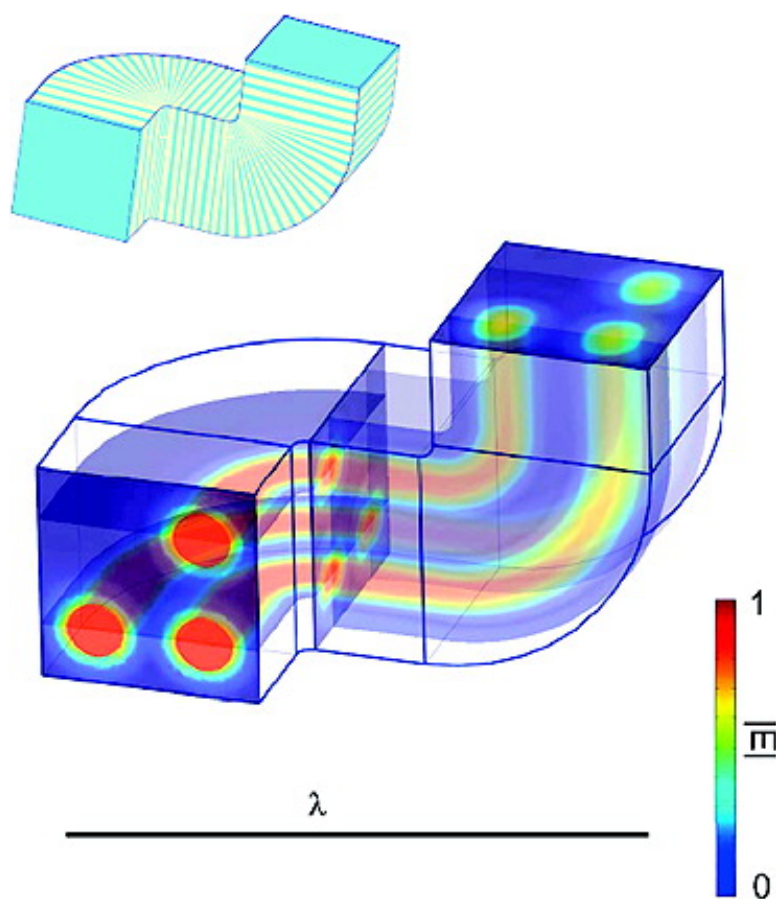


Ray Optics at a Deep-Subwavelength Scale: A Transformation Optics Approach

Seunghoon Han, Yi Xiong, Dentcho Genov, Zhaowei Liu, Guy Bartal, and Xiang Zhang

Nano Lett., **2008**, 8 (12), 4243-4247 • Publication Date (Web): 29 October 2008

Downloaded from <http://pubs.acs.org> on December 11, 2008



More About This Article

Additional resources and features associated with this article are available within the HTML version:

- Supporting Information



ACS Publications
High quality. High impact.

NANO LETTERS

Subscriber access provided by UNIV OF CALIFORNIA CDL ACQUISITIONS

- Access to high resolution figures
- Links to articles and content related to this article
- Copyright permission to reproduce figures and/or text from this article

[View the Full Text HTML](#)



ACS Publications
High quality. High impact.

Nano Letters is published by the American Chemical Society, 1155 Sixteenth Street N.W., Washington, DC 20036

Ray Optics at a Deep-Subwavelength Scale: A Transformation Optics Approach

Seunghoon Han,[†] Yi Xiong,[†] Dentcho Genov,[†] Zhaowei Liu,[†] Guy Bartal,[†]
and Xiang Zhang^{*,†,‡}

NSF Nanoscale Science and Engineering Center (NSEC), University of California, Berkeley, California 94720, and Materials Sciences Division, Lawrence Berkeley National Laboratory, 1 Cyclotron Road, Berkeley, California 94720

Received July 2, 2008; Revised Manuscript Received September 30, 2008

ABSTRACT

We present a transformation optics approach for molding the light flow at the deep-subwavelength scale, using metamaterials with uniquely designed dispersion. By conformal transformation of the electromagnetic space, we develop a methodology for realizing subwavelength ray optics with curved ray trajectories. This enables deep-subwavelength-scale beams to flow through two- or three-dimensional spaces.

The diffractive nature of light^{1–3} has limited optics and photonics to operate at length scales larger than the wavelength of light. The major challenge in scaling down integrated optics is how to mold the light flow below the diffraction limit in all three dimensions (Figure 1a). A high-index solid-immersion lens⁴ can improve the spatial resolution by increasing the medium refractive index but only to a few times higher than that in air. Photonic crystals^{5–8} can guide light in three dimensions. However, the guided beam width is on the order of a wavelength. Surface plasmons^{9–11} have the potential to reach the subwavelength scales; nevertheless, it is confined in the two-dimensional interface between metals and dielectrics. Here, we introduce the concept of ray optics into the subwavelength scale. By using uniquely designed metamaterials and conformal transformation of the electromagnetic (EM) space, molding the flow of light at the deep-subwavelength scale becomes possible.

Ray optics is a powerful tool for designing and analyzing optical systems by tracing the ray trajectories in the medium according to a simple set of geometrical rules.^{1,2} It is an ideal form of light propagation, where wave-optics phenomena such as diffraction of a narrow beam or wavefront distortion due to variations in the material response are assumed to be negligible. Ray optics is based on the “short-wavelength approximation”: the characteristic lengths associated with both diffraction and material variations are very large compared to the wavelength. Consequently, the flow of light in a three-dimensional space can be realized by mapping the direction of light rays at each

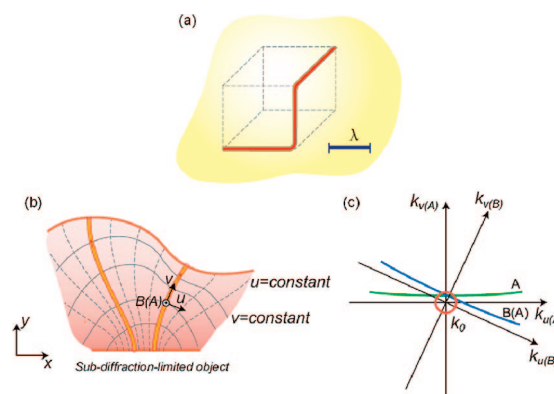


Figure 1. Extending ray optics to the subwavelength scale. (a) Molding light at the subwavelength scale along three-dimensional curved ray trajectories in a metamaterial. (b) Curvilinear representation of the (u, v) axes. The v -axis ($u = \text{constant}$) and u -axis ($v = \text{constant}$) contours are represented by the dashed and solid gray lines, respectively. The light rays follow the v -axis trajectories. Subwavelength-diameter beams (represented by the yellow tubes) can be molded along these trajectories. (c) Near-flat dispersion curves in metamaterials at an arbitrary point A in the Cartesian representation of the (u, v) mesh (green curve) and at the point B(A) in the curvilinear representation of (u, v) with respect to the global coordinates (x, y) (blue curve). The dispersion curve of the vacuum is represented by the orange circle with a radius k_0 .

location, resulting in an orthogonal relationship between rays and geometrical wavefronts.¹

Notwithstanding its significant contribution for numerous applications, ray optics fails to describe light propagation at the scale of or below a wavelength. The dispersion laws in naturally occurring materials limit the range of propagating modes in momentum space and result in a strong diffraction

* E-mail: xiang@berkeley.edu.

[†] University of California.

[‡] Lawrence Berkeley National Laboratory.

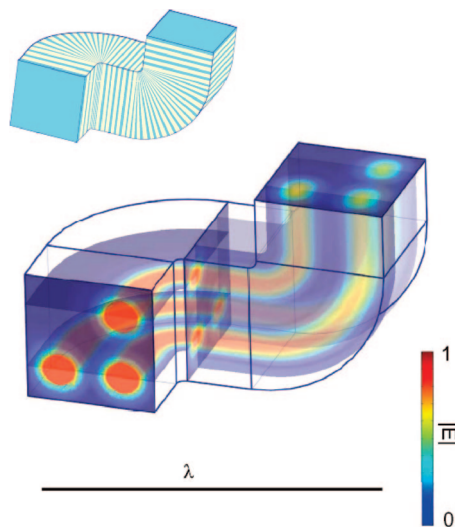


Figure 2. Three-dimensional flow of light at the subwavelength scale. Finite-element calculation of three subwavelength-scale light beams flowing through a metamaterial space represented by an effective medium. The magnitude of the electric field $|E|$ is presented by crosscuts at different orientations. Three constant-amplitude electric field sources of circular shape were situated at the input plane as an arbitrary pattern at the deep-subwavelength scale. The scale bar at the bottom corresponds to a wavelength in free space $\lambda = 589$ nm. The inset illustrates one way to obtain such a metamaterial space by a multilayer design of the effective medium; the blue and white layers correspond to constitutional alternating layers of materials with EM responses of (ϵ_1, μ_1) and (ϵ_2, μ_2) , respectively.

of light because different constituents of a narrow beam propagate with different phase velocities. Moreover, to facilitate light propagation along a wavelength-scale curved trajectory, the host material should have a rapidly varying optical response, which inevitably results in strong wavefront distortion. Consequently, the basic assumptions of ray optics are not valid in these settings. Molding the light flow in the subwavelength scale by means of ray optics necessitates the elimination of diffraction of subwavelength light beams and tailoring of the material properties such that the *effective* optical response varies slowly along propagation.

The emerging field of *metamaterials*^{12–14} has recently provided such means to design artificial materials with unusual optical properties that may not be found in their naturally occurring counterparts. The unit cells in these EM composites can be considerably smaller than the wavelength to describe material properties as an effective homogeneous medium.^{15,16} Metamaterials have shown extraordinary functionalities, such as negative refraction,^{12,17} cloaking of arbitrary objects,^{18,19} and hyperlens,^{20–22} and may pave the way to controlling the diffraction and dispersion of light beams further.

In this paper, we present the concept of *subwavelength ray optics* in a new class of metamaterials having *locally varying* dispersion that is designed to be near flat over a large range in the momentum space ($k_x, k_y \gg 2\pi/\lambda$, λ is the wavelength in a vacuum). The large range of propagating modes in the metamaterial allows the deep-subwavelength size of the beam (without being evanescent), while the near-

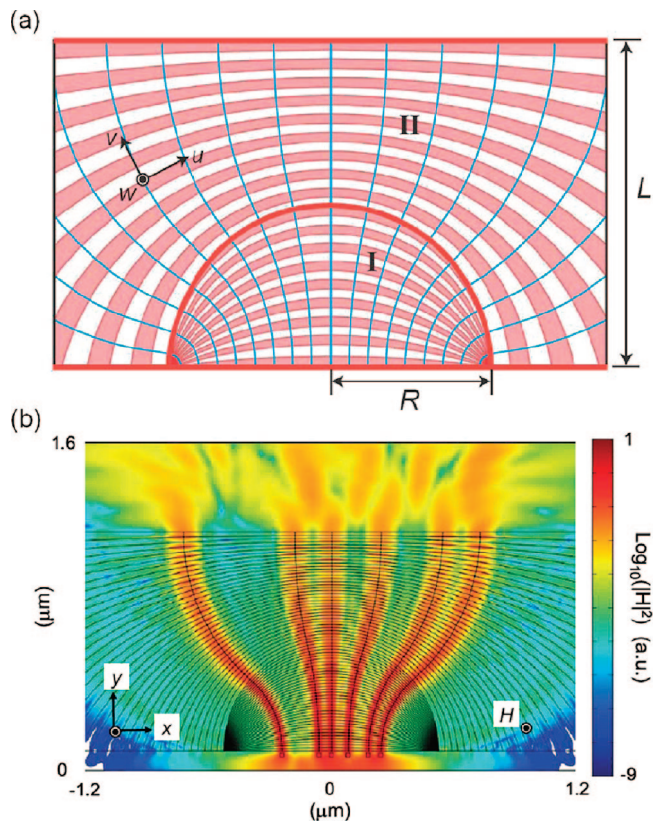


Figure 3. New metamaterial-based optical element: *optical transformer*. (a) Scheme of the optical transformer consisting of two domains of alternating curved layers of Ag (pink) and GaN (white). The light flows along the v axis (curved blue lines), and the interfaces between the layers comply with the u axis. (b) Magnetic field intensity profile showing subwavelength imaging and magnification of the optical transformer.

flat dispersion ensures that these beams do not diffract in the medium because all spatial components propagate with the same phase velocity. The rapidly varying local material response can be engineered such that the effective response is slowly varying in a transformed space. As a result, ray-like light flow becomes feasible in the deep-subwavelength scale similarly to ray optics at much larger scales.^{1,2} Light can propagate throughout two- or three-dimensional space with deep-subwavelength beam profiles, as shown in the following.

We start with a general physical picture in which the concepts of ray optics can be extended to the subwavelength scale. We realize that metamaterials with rapidly varying optical properties can still comply with the ray optics approximations under certain conditions: the existence of an equivalent space, in which the light experiences an effective homogeneous medium along its propagation and flows along *linear* ray trajectories. The invariance of the Maxwell equation under *conformal transformation*²³ ensures that the ray-like behavior will be sustained in the original space, where the light propagates along *curved* ray trajectories (Figure 1b).

In what follows, we introduce the equivalent two-dimensional space, obtained by a conformal transformation

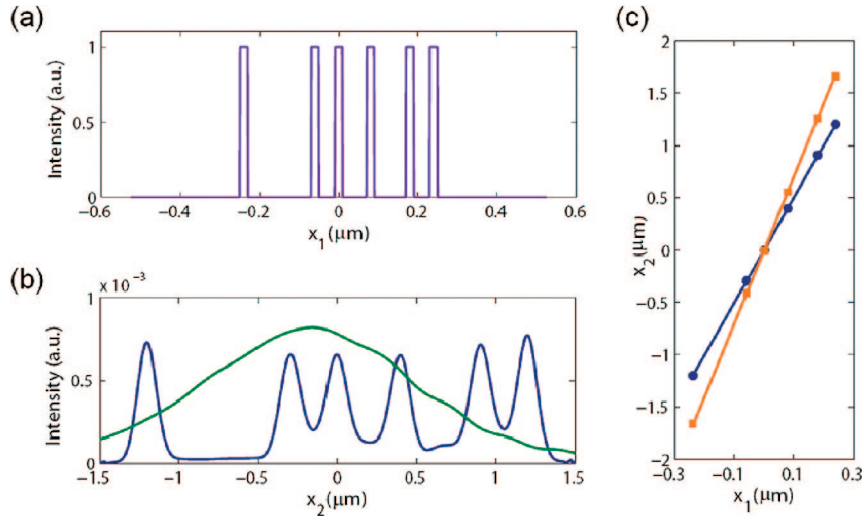


Figure 4. Imaging characteristics of the optical transformer. (a) Intensity distribution of the same arbitrarily spaced subdiffraction-limited objects as those in Figure 3 at the object plane. (b) The same objects magnified by $5\times$ at the image plane of the transformer ($R = 525$ nm, $L = 2115$ nm, blue line) compared with the propagation of the same objects in air (green line, the intensity is scaled by $1/250\times$). (c) Linear imaging characteristics for two different transformers: $5\times$ ($R = 525$ nm, $L = 2115$ nm, presented by the blue line) and $7\times$ ($R = 405$ nm, $L = 2445$ nm, presented by the red line). The circular and square markers correspond to the numerical calculation results. The solid lines are the analytical linear magnifying imaging relations of eq 6.

and represented by the coordinate system (u, v) , which can be easily extended to a three-dimensional space by translation or rotation.²³ The light flows in the form of ray trajectories along the v axis (Figure 1b). We define $\vec{s} = (\varepsilon, \mu)$ and $\vec{s}' = (\varepsilon', \mu')$ to be the diagonalized constituents of the permittivity and permeability along the (u, v, w) axes in the Cartesian and curvilinear representations of (u, v, w) , respectively (e.g., Figures S1 and S2 in the Supporting Information). The relations between \vec{s} and \vec{s}' are given by

$$s'_u = s_u \frac{1}{h_u}, \quad s'_v = s_v \frac{1}{h_v}, \quad s'_w = s_w \frac{h_w}{h_u h_v} \quad (1)$$

where

$$h_u^2 = h_v^2 = \left(\frac{\partial x}{\partial u}\right)^2 + \left(\frac{\partial y}{\partial u}\right)^2, \quad h_w^2 = \left(\frac{\partial z}{\partial w}\right)^2 \quad (2)$$

are the Lamé coefficients.¹⁸ The degeneracy ($h_u = h_v$) originates from the Cauchy–Riemann relationships ($\partial x/\partial u = \partial y/\partial v$, $\partial x/\partial v = -\partial y/\partial u$)²³ and simplifies the design and analysis of the optical system.

A diffraction-free propagation throughout the medium requires dispersion relations $k_v(k_u)$, where the v axis is the light flow direction, in the form of

$$k_v^2 = \varepsilon \mu \mu_u \left(\frac{\omega^2}{c^2} - \frac{1}{\varepsilon \mu \mu_v} k_u^2 \right), \quad \varepsilon \mu \mu_u = \varepsilon_w \mu_u / h_u^2 > 0 \text{ and} \\ (\varepsilon \mu \mu_v = \varepsilon_w \mu_v / h_v^2 \rightarrow +\infty \text{ or } \mu'_u / \mu'_v = \mu_u / \mu_v \rightarrow -0) \quad (3a)$$

for TE (electric field along the w axis) and

$$k_v^2 = \varepsilon \mu \mu_w \left(\frac{\omega^2}{c^2} - \frac{1}{\varepsilon \mu \mu_w} k_u^2 \right), \quad \varepsilon \mu \mu_w = \varepsilon_u \mu_w / h_u^2 > 0 \text{ and} \\ (\varepsilon \mu \mu_w = \varepsilon_u \mu_w / h_u^2 \rightarrow +\infty \text{ or } \varepsilon'_u / \varepsilon'_v = \varepsilon_u / \varepsilon_v \rightarrow -0) \quad (3b)$$

for TM (magnetic field along the w axis) polarizations.^{15,16} The propagation constant k_v should be near flat over a large range in the transverse momentum k_u , in both the Cartesian and the curvilinear representations of (u, v, w) (see Figure

1c). This condition can also be applied to the (v, w) plane to ensure ray-like propagation in all three dimensions.

By using the above methodology, metamaterial-based optical elements can be designed to mold light at the subwavelength scale and in all three spatial dimensions. This unusual manipulation of light is carried out by cascading multiple metamaterials-based elements with the ability to direct light or bend it by 90° . The 90° bending elements are designed using a circular cylindrical coordinate transformation with rotation about the w axis²³

$$x + iy = \exp(u + iv) \quad u \in (u_1, u_2), v \in (0, \pi/2) \quad (4)$$

where u_1 and u_2 correspond to the internal and external radii of the bends. A uniaxial near-flat local dispersion (eq 3a,b) enables the confinement of the subwavelength beam profiles along both the u and w dimensions during propagation. Such an EM material response can be obtained, e.g., by an effective medium^{15,20,21} composed of thin layers of alternating different materials (blue and white layers in the inset of Figure 2), which provide $s'_u = s'_w = ps_1 + (1-p)s_2$ and $s'_v = s_1 s_2 / [(1-p)s_1 + ps_2]$. $s_1 = (\varepsilon_1, \mu_1)$ and $s_2 = (\varepsilon_2, \mu_2)$ represent the material response of the two media composing the layered structure, where p is the filling fraction of layer 1.

A full-wave simulation using a finite-element solver (COMSOL Multiphysics) shows the applicability of our methodology. Anisotropic effective medium parameters were directly implemented to represent bulk metamaterial as an inset in Figure 2 (Figure S1 in the Supporting Information). Thin multilayers made up of positive index material ($\varepsilon_1 = 2$, $\mu_1 = 1$, e.g., glass) and negative index material ($\varepsilon_2 = -1.98 + 0.02i$, $\mu_2 = -0.99 - 0.01i$) were considered with the filling ratio p set as 1:2. Regarding the constitutional low-loss homogeneous negative index material, there are several indications that it can be obtained at optical frequencies and at atomic/molecular levels.^{24–28} Figure 2

displays ray-like light flow of three beams along complex three-dimensional paths inside the metamaterial. The beam profiles form an arbitrary deep-subwavelength pattern with beam diameter $\lambda/10$ and center-to-center distance between beams $\lambda/5$, where the free-space wavelength $\lambda = 589$ nm was applied in the simulation.^{26,27} A scattering boundary condition has been applied at the external boundaries to absorb outgoing waves from the simulation domain. Despite the beams' deep-subwavelength profiles, the diffraction is suppressed to maintain the beam shapes throughout propagation. Only a relatively small reduction ($\sim 30\%$) in the peak amplitude is observed at the output. This contrasts with the case of conventional dielectric waveguides (e.g., glass core ($\epsilon_{\text{core}} = 2, \mu_{\text{core}} = 1$) and air surrounding ($\epsilon_{\text{clad}} = 1, \mu_{\text{clad}} = 1$)), where such deep-subwavelength profiles cannot propagate in the dielectric medium and hence form evanescent waves.¹⁻³ While some waveguides can be specially designed to reduce their mode areas,^{10,29} they support only a fixed single-mode profile and subwavelength bending in three-dimensional space such as in Figure 2 is unattainable. A multimode fiber bundle (fiber-optic image conduit) can deliver arbitrarily shaped beams, but its structures and beam profiles are considerably larger than the wavelength utilizing the traditional ray optics limit (i.e., short-wavelength approximation).

As an actual demonstration of the methodology, we develop an optical “transformer” that can project images of deep-subwavelength objects to far field (or in reverse) between flat input and output planes with negligible distortion. Such a metamaterial optical element is constructed by layers of metal and dielectric, forming two domains (I and II) of cylindrically symmetric curvilinear orthogonal coordinates. In Figure 3a, the coordinates are represented by the blue lines (v axis) and the interfaces between the layers (u axis). Such curvilinear coordinates are mapped onto the Cartesian space (x, y, z) through bipolar transformations²³

$$\begin{aligned} x - iy &= R \coth\left(\frac{u_1 + iv_1}{2}\right) \quad \text{for region I,} \\ u_1 &\in (-\infty, \infty), v_1 \in (\pi/2, \pi) \\ y + ix &= L - \sqrt{L^2 - R^2} \coth\left(\frac{v_2 + iu_2}{2}\right) \quad \text{for region II,} \\ u_2 &= 2 \tan^{-1}\left(\tanh\left(\frac{v_{R,L}}{2}\right) \coth\left(\frac{u_1}{2}\right)\right), v_2 \in (0, v_{R,L}) \end{aligned} \quad (5)$$

where $v_{R,L} = 2 \tanh^{-1}(\sqrt{(L-R)/(L+R)})$, L and R are the length and inner radius of the element, respectively, and the cylindrical symmetry imposing $z = w$ for both regions (Figure S2 in the Supporting Information). The ray trajectories conform to the curved v axis (constant u), providing magnifying imaging with linear relations

$$x_2 = mx_1, m = 1 + \frac{L}{R} \quad (6)$$

where x_1 and x_2 are the lateral sizes of the object at the bottom plane and image at the top plane of the element, respectively. The magnification factor m is determined solely by the geometrical relation between L and R ; hence, it is fully controlled by the design of the optical element.

We have simulated the actual imaging of a set of arbitrarily spaced subdiffraction-limited objects of size $\sim \lambda/20$, placed at the bottom of the transformer (Figure 3b). The optical element is made of alternating Ag ($\epsilon_{\text{Ag}} = -6.067 + 0.197i$) and GaN ($\epsilon_{\text{GaN}} = 6.088$) curved layers, where the metal–dielectric interfaces comply with the $v = \text{constant}$ contours. The element is surrounded by GaN. The operating free-space wavelength λ is 431 nm. Several advanced fabrications^{30,31} may enable one to achieve such a profile.

The local anisotropic response is determined by the effective medium parameters $\epsilon'_v = \epsilon_{\text{Ag}}\epsilon_{\text{GaN}}/[p\epsilon_{\text{GaN}} + (1 - p)\epsilon_{\text{Ag}}]$, $\epsilon'_u = p\epsilon_{\text{Ag}} + (1 - p)\epsilon_{\text{GaN}}$, and $\mu'_w = 1$. For TM polarization, by keeping the filling fraction as $p = 1/2$ over the entire space, the conditions of near-flat dispersion and a slowly varying effective material response are satisfied, enabling the use of ray tracing for imaging objects of a size as small as $\lambda/20$. Clearly, despite the deep-subwavelength profiles of the objects, the magnetic intensity flow of Figure 3b shows that the image is projected onto the output face with $3\times$ magnification, with minimal distortion and relative -11 dB loss.

To generalize the imaging characteristics, a subdiffraction-limited object, shown in Figure 4a, is imaged to the far field by a $5\times$ magnifying transformer with air surroundings (blue line in Figure 4b). At the input and output planes of the transformer, thin GaN layers were added to enhance the impedance matching and, hence, the overall transmittance. On the contrary, the numerical “control experiment” of the same object propagating in free space results in a broad bell-shaped field distribution, with no resemblance to the original object (green line in Figure 4b). Namely, only a small fraction of low-resolution spatial information is transferred, whereas the information of fine features, carried by the evanescent fields, cannot propagate. The relatively large loss (-24 dB) of the transformer may be further reduced for practical applications by finding low-loss negative index materials^{25,26} or introducing gain.²⁷ Considering reverse light propagation from the far field to generate arbitrary deep-subwavelength patterns at the bottom of the transformer, the current amount of loss could be tolerable for other applications like subwavelength optical tweezers.³² Figure 4c depicts the linear imaging relations between the object and image positions (eq 6), where the ratio between the displacement of a point object at the image plane and its displacement at the object plane remains constant in all cases.

In conclusion, we demonstrated a new approach of ray optics at the deep-subwavelength scale, using metamaterials with properly designed dispersion characteristics. The new methodology combines near-flat dispersion and conformal transformation to obtain an equivalent space, represented by curvilinear orthogonal coordinates. In this space, the material response is effectively slowly varying to maintain ray properties. Using this methodology, we have shown a ray-like flow of light with beam width at a scale of $\lambda/10$ in the metamaterial-based elements. Subwavelength ray optics offers new exciting possibilities in science and technology

applications such as high-density integrated optics, nanoscale optical microscopy/lithography, and subwavelength optical tweezers.

Acknowledgment. This work was mainly supported by the U.S. Department of Energy under Contract DE-AC02-05CH11231, and in partial support from the NSF Centre for Scalable and Integrated Nano Manufacturing (SINAM) (Grant No. DMI-0327077). Dr. S. Han thanks the support from the Korea Research Foundation Grant funded by the Korean Government, KRF-2006-214-D00119.

Supporting Information Available: Conformal transformation of the metamaterial optical elements and related renormalization of their material parameters. This material is available free of charge via the Internet at <http://pubs.acs.org>.

References

- (1) Born, M.; Wolf, E. *Principles of Optics*; Cambridge University Press: Cambridge, U.K., 1999.
- (2) Saleh, B. E. A.; Teich, M. C. *Fundamentals of Photonics*; Wiley: New York, 1991.
- (3) Goodman, J. W. *Introduction to Fourier Optics*; McGraw-Hill: New York, 1996.
- (4) Mansfield, S. M.; Kino, G. S. *Appl. Phys. Lett.* **1990**, *57*, 2615.
- (5) Yablonovitch, E. *Phys. Rev. Lett.* **1987**, *58*, 2059.
- (6) Joannopoulos, J. D.; Meade, R. D.; Winn, J. N. *Photonic Crystals*; Princeton University: New York, 1995.
- (7) Chow, E.; et al. *Nature* **2000**, *407*, 983.
- (8) Mekis, A.; Chen, J. C.; Kurland, I.; Fan, S.; Villeneuve, P. R.; Joannopoulos, J. D. *Phys. Rev. Lett.* **1996**, *77*, 3787.
- (9) Barnes, W. L.; Dereux, A.; Ebbesen, T. W. *Nature* **2003**, *424*, 824.
- (10) Ozbay, E. *Science* **2006**, *311*, 189.
- (11) García-Vidal, F. J.; Lezec, H. J.; Ebbesen, T. W.; Martín-Moreno, L. *Phys. Rev. Lett.* **2003**, *90*, 213901.
- (12) Pendry, J. B. *Phys. Rev. Lett.* **2000**, *85*, 3966.
- (13) Soukoulis, C. M.; Linden, S.; Wegener, M. *Science* **2007**, *315*, 47.
- (14) Shalaev, V. M. *Nat. Photonics* **2007**, *1*, 41.
- (15) Ramakrishna, S. A.; Pendry, J. B.; Wiltshire, M. C. K.; Stewart, W. J. *J. Mod. Opt.* **2003**, *50*, 1419.
- (16) Smith, D. R.; Schurig, D. *Phys. Rev. Lett.* **2003**, *90*, 077405.
- (17) Fang, N.; Lee, H.; Sun, C.; Zhang, X. *Science* **2005**, *308*, 534.
- (18) Pendry, J. B.; Schurig, D.; Smith, D. R. *Science* **2006**, *312*, 1780.
- (19) Cai, W.; Chettiar, U. K.; Kildishev, A. V.; Shalaev, V. M. *Nat. Photonics* **2007**, *1*, 224.
- (20) Salandrino, A.; Engheta, N. *Phys. Rev. B* **2006**, *74*, 075103.
- (21) Jacob, Z.; Alekseyev, L. V.; Narimanov, E. *Opt. Express* **2006**, *14*, 8247.
- (22) Liu, Z.; Lee, H.; Xiong, Y.; Sun, C.; Zhang, X. *Science* **2007**, *315*, 1686.
- (23) Moon, P.; Spencer, D. E. *Field Theory Handbook*; Springer-Verlag: New York, 2007.
- (24) Oktel, M. Ö.; Müstecaplıoğlu, Ö. E. *Phys. Rev. A* **2004**, *70*, 053806.
- (25) Oliveira, S. L.; Rand, S. C. *Phys. Rev. Lett.* **2007**, *98*, 093901.
- (26) Kästel, J.; Fleischhauer, M.; Juzeliūnas, G. *Phys. Rev. A* **2007**, *76*, 062509.
- (27) Krowne, C. M. *Phys. Lett. A* **2008**, *372*, 2304.
- (28) Radovanovic, P. V.; Barrelet, C. J.; Gradecak, S.; Qian, F.; Lieber, C. M. *Nano Lett.* **2005**, *5*, 1407.
- (29) Robinson, J. T.; Manolatu, C.; Chen, L.; Lipson, M. *Phys. Rev. Lett.* **2005**, *95*, 143901.
- (30) Wonisch, A.; et al. *Appl. Opt.* **2006**, *45*, 4147.
- (31) Zhang, J.; You, L.; Ye, H.; Yu, D. *Nanotechnol.* **2008**, *18*, 155303.
- (32) Righini, M.; Zelenina, A.; Girard, C.; Quidant, R. *Nat. Phys.* **2007**, *3*, 477.

NL801942X